Macromolecules

Article

Cite This: *Macromolecules* 2018, 51, 9011−9018

pubs.acs.org/Macromolecules

Analysis of Small-Angle Neutron Scattering Spectra from Deformed Polymers with the Spherical Harmonic Expansion Method and a Network Model

Zhi-Yuan Wang,[†,‡] Dejia Kong,[†,‡] Lincan Yang,[§] Hongwei Ma,[*,§] Fengmei Su,[∥] Kanae Ito,[⊥] Yun Liu,[⊥] Xuewu Wang,[†,‡] and Zhe Wang[*,†,‡]

[†]Department of Engineering Physics and [‡]Key Laboratory of Particle & Radiation Imaging, Ministry of Education, Tsinghua University, Beijing 100084, China

[§]Department of Polymer Science and Engineering, School of Chemical Engineering, Dalian University of Technology, Dalian, Liaoning 116024, China

[∥]National Engineering Research Center for Advanced Polymer Processing Technology, Key Laboratory of Advanced Materials Processing & Mold (Zhengzhou University), Ministry of Education, Zhengzhou University, Zhengzhou, Henan 450002, China

[⊥]Center for Neutron Research, National Institute of Standards and Technology, Gaithersburg, Maryland 20899-6100, United States

ABSTRACT: We combine the recently proposed spherical harmonic expansion (SHE) method [*Phys. Rev. X* **2017**, 7, 031003] with a modified network model to analyze the small-angle neutron scattering (SANS) spectra from deformed entangled polymers. Focusing on the leading anisotropic component and the isotropic component in the SHE, the analysis gives a reliable value of the stretch ratio of the end-to-end vector, and a reasonable estimation of the radius of gyration, of a single chain in polymers undergoing uniaxial deformation and relaxation. Moreover, it provides a practical way to evaluate the stress of deformed entangled polymers with the SANS spectra from a viewpoint of rubber elasticity.

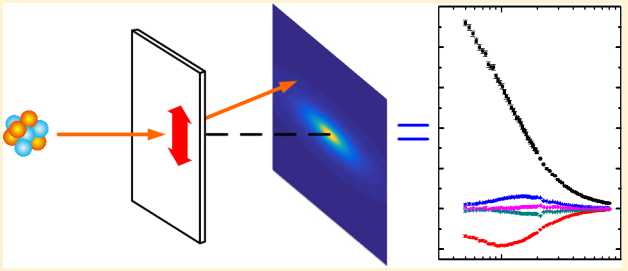

I. INTRODUCTION

The study of the microscopic structure and dynamics of polymeric systems has been greatly promoted by the use of small-angle neutron scattering (SANS). By mixing protonated chains with selectively deuterated counterparts, it can extract the form factor of the labeled path.[1] From the 1980s, extensive SANS investigations have been made in illustrating the molecular conformation of deformed linear polymers based on the concept of "tube", which was proposed by de Gennes, Doi, and Edwards[2,3] to give an elegant treatment on the entanglement effect. For example, Pyckhout-Hintzen and collaborators systematically investigated the microscopic strain and the deformation of tube in polymer networks.[4−8] Blanchard et al.[9] and Boué et al.[10,11] tested the prediction of the tube model on the chain relaxation with uniaxially strained entangled polymers. In addition, some other models, such as the network model[12,13] and modified Debye model,[14] have also been employed to find the chain conformation in deformed polymer networks and entangled polymers.

Recently, we have proposed a model-independent framework, the spherical harmonic expansion (SHE) method, for the investigation of molecular deformation with uniaxial symmetry.[15] In this method, the anisotropic two-dimensional (2D) spectrum of deformed polymers is decomposed into several one-dimensional (1D) Q-dependent coefficients ($\mathbf{Q}$ is the scattering vector in the SANS experiment). Each coefficient has a specific symmetry and thus contains unique physical significance. In this work, to further extract detailed structural information about deformed entangled polymers at the molecular level, we extend the SHE method to the real space and combine it with a modified network model to analyze the SANS spectra. The result shows that by analyzing the leading anisotropic coefficient and the isotropic coefficient, it can find the strain and the radius of gyration of a single chain. Moreover, it provides a practical way to estimate the stress from the SANS spectra through the viewpoint of rubber elasticity.

The rest of this paper is organized as follows. In section II, we first give a brief review on the SHE method and point out the expressions connecting the expansion coefficients of the SANS spectrum and those of the distribution function. The physical significances of the first two coefficients are emphasized. Then we introduce the modified network model for analyzing the SANS data from deformed entangled polymers. Section III provides the properties of the sample and some details of the SANS experiment. Section IV describes the analysis results. Concluding remarks are included in section V.

Received: September 5, 2018
Revised: October 1, 2018
Published: October 31, 2018

DOI: 10.1021/acs.macromol.8b01913
Macromolecules 2018, 51, 9011−9018

II. THEORETICAL BACKGROUND

Spherical Harmonic Expansion Method. Here we briefly review the SHE method and introduce the relations connecting the expansion coefficients in real space and those in reciprocal space for the study of uniaxially deformed polymers. The polymer chain can be modeled as a series of N segments. The position of the ith segment is denoted as $\mathbf{r}_i$. The single-chain structure factor, which characterizes the conformation of a polymer chain, is defined as

$$S(\mathbf{Q}) = \frac{1}{N^2}\langle \sum_{i,j}^{N} e^{-i\mathbf{Q}\cdot(\mathbf{r}_i-\mathbf{r}_j)}\rangle \tag{1}$$

where $\mathbf{Q}$ is the scattering wave vector and $\langle ...\rangle$ denotes the ensemble average. For polymer melts, $S(\mathbf{Q})$ can be obtained from SANS experiments by measuring a mixture of deuterated chains and protonated chains at the same molecular weight. The coherent SANS spectrum of this mixture, $I(\mathbf{Q})$, is expressed as[1]

$$I(\mathbf{Q}) = n(b_D - b_H)^2 N^2 x(1-x)S(\mathbf{Q}) \tag{2}$$

where n is the number density of polymer chains, $(b_D - b_H)$ is the contrast of scattering length between the deuterated and protonated segments, and x is the fraction of the deuterated chains. $S(\mathbf{Q})$ is determined by the segment distribution function $\psi(i,j;\mathbf{r})$. $\psi(i,j;\mathbf{r})\mathrm{d}\mathbf{r}$ gives the probability of finding the jth segment at distance $\mathbf{r}$ from the ith segment in the volume element $\mathrm{d}\mathbf{r}$. With $\psi(i,j;\mathbf{r})$, it can define the intrachain pair distribution function $g(\mathbf{r})$:

$$g(\mathbf{r}) = \frac{1}{N^2}\sum_{i,j}^{N}\psi(i,j;\mathbf{r}) \tag{3}$$

$g(\mathbf{r})$ and $S(\mathbf{Q})$ are related by the Fourier transform:

$$S(\mathbf{Q}) = \int g(\mathbf{r})e^{-i\mathbf{Q}\cdot\mathbf{r}}\,\mathrm{d}\mathbf{r} \tag{4}$$

The $S(\mathbf{Q})$ of a deformed polymer is anisotropic. It can be expanded with spherical harmonics:

$$S(\mathbf{Q}) = \sum_{l,m} S_l^m(Q)Y_l^m(\mathbf{\Omega}) \tag{5}$$

where $S_l^m(Q)$ is the expansion coefficient and $Y_l^m(\mathbf{\Omega})$ is the (real) spherical harmonic function defined as

$$Y_l^m(\mathbf{\Omega}) = Y_l^m(\theta,\phi) = \begin{cases} \sqrt{2}\sqrt{(2l+1)\dfrac{(l-|m|)!}{(l+|m|)!}}P_l^{|m|}(\cos\theta)\sin(|m|\phi) & (m<0) \\ \sqrt{2l+1}\,P_l^0(\cos\theta) & (m=0) \\ \sqrt{2}\sqrt{(2l+1)\dfrac{(l-m)!}{(l+m)!}}P_l^m(\cos\theta)\cos(m\phi) & (m>0) \end{cases} \tag{6}$$

where $P_l^m(x)$ are the associated Legendre polynomials, θ is the polar angle from the positive z-axis, and ϕ is the azimuthal angle in the xy-plane from the positive x-axis.

For the uniaxial extension with the stretching direction along z-axis, the $S(\mathbf{Q})$ has an axial symmetry. It can be found that all terms with odd l and $m \neq 0$ are forbidden, which leads to the following expansion:[15]

$$S(\mathbf{Q}) = \sum_{l:\mathrm{even}} S_l^0(Q)Y_l^0(\mathbf{\Omega}) \tag{7}$$

According to eq 6, $Y_l^0(\mathbf{\Omega})$ (l is even) only depends on $\cos^2\theta$. Figure 1a gives a typical configuration of a SANS experiment on a uniaxially stretched polymer. The direction of incident radiation is parallel to the y-axis. In this case, the scattering intensity given by the 2D detector displays the cross section of $S(\mathbf{Q})$ in the xz-plane, namely, $S(Q_x, Q_y = 0, Q_z)$, or equivalently, $S(Q, \theta, \phi = 0)$. It can be proven that in the xz-plane the orthogonality of $Y_l^0(\mathbf{\Omega})$ is expressed as[15]

$$\int_0^\pi Y_l^0(\theta)Y_{l'}^0(\theta)\sin\theta\,\mathrm{d}\theta = 2\delta_{ll'} \quad (l \text{ and } l' \text{ are even}) \tag{8}$$

Combining the above two equations, it can obtain $S_l^0(Q)$ from the measured $S(Q, \theta, \phi = 0)$ by the following equation:[15]

$$S_l^0(Q) = \frac{1}{2}\int_0^\pi S(Q,\theta,\phi=0)Y_l^0(\theta)\sin\theta\,\mathrm{d}\theta \tag{9}$$

Figures 1b and 1c give the 2D cross section of $S(\mathbf{Q})$ at the xz-plane and the 1D expansion coefficients $S_l^0(Q)$ for a Gaussian chain undergoing an affine uniaxial elongation with a stretch ratio of 2, respectively.

Under a uniaxial deformation, $g(\mathbf{r})$ and $\psi(i,j;\mathbf{r})$ have similar expansions:

$$g(\mathbf{r}) = \sum_{l:\mathrm{even}} g_l^0(r)Y_l^0(\theta) \tag{10}$$

$$\psi(i,j;\mathbf{r}) = \sum_{l:\mathrm{even}} \psi_l^0(i,j;r)Y_l^0(\theta) \tag{11}$$

$S_l^0(Q)$ and $g_l^0(r)$ are related by the Bessel transform:

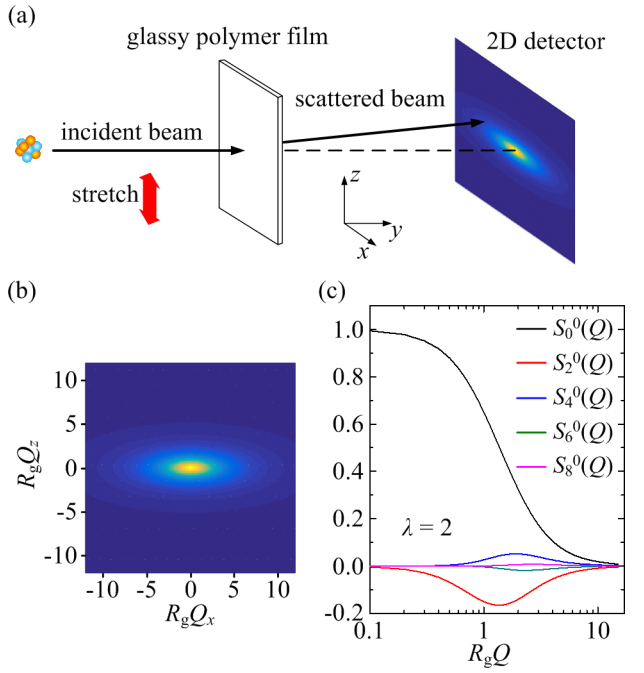

Figure 1. Panel a gives the illustration of the SANS experiment on the uniaxially stretched polymers. Panels b and c display the simulated 2D spectrum $S(\mathbf{Q})$ and the corresponding 1D coefficients $S_l^0(Q)$ for a Gaussian chain under an affine elongation with the stretch ratio of 2, respectively.

DOI: 10.1021/acs.macromol.8b01913
Macromolecules 2018, 51, 9011−9018

$$S_l^0(Q) = i^l 4\pi \int_0^\infty g_l^0(r) J_l(Qr) r^2 \, dr \tag{12}$$

$$g_l^0(r) = \frac{i^l}{2\pi^2} \int_0^\infty S_l^0(Q) J_l(Qr) Q^2 \, dQ \tag{13}$$

where $J_l(x)$ is the l-order spherical Bessel function. $g_l^0(r)$ and $\psi_l^0(i,j;r)$ are related as follows:

$$g_l^0(r) = \frac{1}{N^2} \sum_{i,j}^{N} \psi_l^0(i, j; r) = \frac{1}{N^2} \int_0^N di \int_0^N dj \, \psi_l^0(i, j; r) \tag{14}$$

Generally, $\psi(i,j;\mathbf{r})$ only depends on $|i - j|$. Thus, the preceding equation can be rewritten as

$$g_l^0(r) = \frac{2}{N^2} \int_0^N di \int_0^i dj \, \psi_l^0(|i - j|, r) = \frac{2}{N^2} \int_0^N dt \times \psi_l^0(t, r)(N - t) \tag{15}$$

where $\psi_l^0(|i - j|, r) = \psi_l^0(i,j;r)$.

With eqs 15 and 12, it can transform the components of the distribution function to those of $S(\mathbf{Q})$.

$S_0^0(\mathbf{Q})$ and $S_2^0(\mathbf{Q})$. As we shall see, the isotropic term, $S_0^0(Q)$, and the leading anisotropic term, $S_2^0(Q)$, have significant physical meanings.

The mean-square radius of gyration of a polymer chain R_g^2 is defined as[3]

$$R_g^2 = \frac{1}{2N^2} \sum_{i,j=1}^{N} \langle (\mathbf{r}_i - \mathbf{r}_j)^2 \rangle \tag{16}$$

where $\langle (\mathbf{r}_i - \mathbf{r}_j)^2 \rangle$ can be expressed as

$$\langle (\mathbf{r}_i - \mathbf{r}_j)^2 \rangle = \int \mathbf{r}^2 \psi(i, j; \mathbf{r}) \, d\mathbf{r} \tag{17}$$

With eqs 8 and 11, it is straightforward to show that

$$\langle (\mathbf{r}_i - \mathbf{r}_j)^2 \rangle = 4\pi \int_0^\infty r^4 \psi_0^0(i, j; r) \, dr \tag{18}$$

Then R_g^2 is expressed as

$$R_g^2 = \frac{2\pi}{N^2} \sum_{i,j=1}^{N} \int_0^\infty r^4 \psi_0^0(i, j; r) \, dr = 2\pi \int_0^\infty r^4 g_0^0(r) \, dr \tag{19}$$

It is seen that R_g can be solely determined from $S_0^0(Q)$.

$Y_2^0(\theta)$ has the same symmetry as the geometry of uniaxial extension. Therefore, $S_2^0(Q)$ is the most relevant quantity that relates to the deformation of polymers.[15] It was pointed out that the tensile stress solely depends on $S_2^0(Q)$ (or ψ_2^0).[16] The stress tensor is expressed as follows:[3,17]

$$\vec{\sigma} = 2k_B T n \beta^2 \int \mathbf{R}\mathbf{R} \psi \, d\mathbf{R} \tag{20}$$

where n is the number density of chains, $\mathbf{R}$ is the end-to-end vector of a chain, ψ is the distribution function of $\mathbf{R}$, β is expressed as $\beta = (3/2Nb^2)^{1/2}$, and b is the average bond length between two adjacent segments. Under the condition of uniaxial extension along the z-axis, the tensile stress is written as

$$\sigma_{zz} - \sigma_{xx} = 2k_B T n \beta^2 \int (R_z^2 - R_x^2) \sum_{l:\text{even}} \psi_l^0(R) \times Y_l^0(\theta) R^2 dR \sin\theta \, d\theta \, d\phi \tag{21}$$

Replacing R_z and R_x by $R\cos\theta$ and $R\sin\theta\cos\phi$, and then applying eq 8, one can find the following relation, which has been given in a recent publication:[16]

$$\sigma_{zz} - \sigma_{xx} = \frac{8\pi}{\sqrt{5}} n k_B T \beta^2 \int R^4 \psi_2^0(R) \, dR \tag{22}$$

Nonaffine Network Model for Entangled Polymers. It is well-accepted that polymer melts will be in an entangled state when the molecular weight is higher than a critical value.[3,17,18] In this case, each chain entangles with other chains physically. The portion of polymer between two neighboring points of entanglement is called a strand. Because the segment distribution within a strand depends on the end-to-end vector of this strand, it is useful to introduce the conditional segment distribution function $W(i,j;\mathbf{r},\mathbf{R}_s)$, which gives the probability that segments i and j are separated by $\mathbf{r}$ under the condition that the strand ends are separated by $\mathbf{R}_s$. Ullman found a bivariate Gaussian form for $W(i,j;\mathbf{r},\mathbf{R}_s)$ for a Gaussian chain:[12]

$$W(i, j; \mathbf{r}, \mathbf{R}_s) = \left[\frac{3}{2\pi N_s b^2 w_{ij}(1 - w_{ij})} \right]^{3/2} \times \exp\left[-\frac{3}{2N_s b^2 w_{ij}(1 - w_{ij})} (\mathbf{r} - w_{ij}\mathbf{R}_s)^2 \right] \tag{23}$$

where N_s is the segment number of a strand, and $w_{ij} = |i - j|/N_s$. With eq 23, the segment distribution function $\psi(i,j;\mathbf{r})$, which describes the distribution of two segments i and j within a strand, can be written as

$$\psi(i, j; \mathbf{r}) = \int W(i, j; \mathbf{r}, \mathbf{R}_s) \psi(\mathbf{R}_s) \, d\mathbf{R}_s \tag{24}$$

where $\psi(\mathbf{R}_s)$ is the distribution function of $\mathbf{R}_s$. $\psi(\mathbf{R}_s)$ has a Gaussian form for a Gaussian chain:

$$\psi(\mathbf{R}_s) = \left(\frac{3}{2\pi N_s b^2} \right)^{3/2} \exp\left[-\frac{3}{2N_s b^2} \left(\frac{R_{s,x}^2}{\lambda_x^2} + \frac{R_{s,y}^2}{\lambda_y^2} + \frac{R_{s,z}^2}{\lambda_z^2} \right) \right] \tag{25}$$

where λ_i $(i = x, y, z)$ denotes the strain of the end-to-end vector of the strand at each direction. Combining the preceding three equations, one can obtain that

$$\psi(i, j; \mathbf{r}) = \left(\frac{\beta_s^2}{\pi w_{ij}} \right)^{3/2} \sqrt{\frac{1}{(w_{ij}\lambda_x^2 + 1 - w_{ij})(w_{ij}\lambda_y^2 + 1 - w_{ij})(w_{ij}\lambda_z^2 + 1 - w_{ij})}} \times \exp\left[-\frac{\beta_s^2}{w_{ij}} \left(\frac{r_x^2}{w_{ij}\lambda_x^2 + 1 - w_{ij}} + \frac{r_y^2}{w_{ij}\lambda_y^2 + 1 - w_{ij}} + \frac{r_z^2}{w_{ij}\lambda_z^2 + 1 - w_{ij}} \right) \right] \tag{26}$$

where $\beta_s^2 = 3/2N_s b^2$. The preceding equation gives the segment distribution function for the case that i and j are within one strand.

For the case of $|i - j| \gg N_s$, the constraint of the strand is no longer important; $\psi(i,j;\mathbf{r})$ reduces to a simple Gaussian form for a Gaussian chain:

DOI: 10.1021/acs.macromol.8b01913
Macromolecules 2018, 51, 9011−9018

$$\psi(i, j; \mathbf{r}) = \left(\frac{3}{2\pi|i-j|b^2}\right)^{3/2} \times \exp\left[-\frac{3}{2|i-j|b^2}\left(\frac{{r_x}^2}{{\lambda_x}^2} + \frac{{r_y}^2}{{\lambda_y}^2} + \frac{{r_z}^2}{{\lambda_z}^2}\right)\right] \tag{27}$$

As $|i-j|$ increases, the expression of $\psi(i,j;\mathbf{r})$ should undergo a crossover from eq 26 to eq 27. For simplicity, we assume that $\psi(i,j;\mathbf{r})$ is expressed by eq 26 at $|i-j| \le N_s$ and by eq 27 at $|i-j| > N_s$.

Under the uniaxial extension along the z-axis, we have $\lambda_x = \lambda_y = 1/\sqrt{\lambda}$ and $\lambda_z = \lambda$, where λ is the stretch ratio along the z-axis. Thus, $\psi(i,j;\mathbf{r})$ has the following form:

$$\psi(i, j; \mathbf{r}) = \left(\frac{\beta_s^2}{\pi w_{ij}}\right)^{3/2} \times \sqrt{\frac{1}{(w_{ij}/\lambda + 1 - w_{ij})(w_{ij}/\lambda + 1 - w_{ij})(w_{ij}\lambda^2 + 1 - w_{ij})}} \times \exp\left[-\frac{\beta_s^2}{w_{ij}}\left(\frac{{r_x}^2}{w_{ij}/\lambda + 1 - w_{ij}} + \frac{{r_y}^2}{w_{ij}/\lambda + 1 - w_{ij}} + \frac{{r_z}^2}{w_{ij}\lambda^2 + 1 - w_{ij}}\right)\right], \quad |i-j| \le N_s \tag{28}$$

$$\psi(i, j; \mathbf{r}) = \left(\frac{3}{2\pi|i-j|b^2}\right)^{3/2} \times \exp\left[-\frac{3}{2|i-j|b^2}\left(\lambda{r_x}^2 + \lambda{r_y}^2 + \frac{{r_z}^2}{\lambda^2}\right)\right], \quad |i-j| > N_s \tag{29}$$

The relaxation times at various length scales can be quite different. Intuitively, the structures with small length scales relax faster than those at large length scales. Therefore, a constant λ is not sufficient to give a complete description on the deformation of a chain at all length scales. In fact, SANS experiments have confirmed the length-scale dependence of deformation in polymeric systems.[7,8,19] To account for this inhomogeneity, here we introduce a microscopic strain λ_{ij}. It is a statistical quantity that characterizes the stretch ratio of $\mathbf{r}_{ij}$, where $\mathbf{r}_{ij}$ is the distance vector between segments i and j at $|i-j| > N_s$. Generally, the dependence of λ_{ij} on $|i-j|$ should be smooth and monotonically increasing. We tentatively assume the expression of λ_{ij} as follows:

$$\lambda_{ij} = \lambda_0 + (\lambda_1 - \lambda_0)\left[1 - \exp\left(-\mu\frac{u_{ij} - 1/Z}{1 - u_{ij}}\right)\right], \quad |i-j| > N_s \tag{30}$$

where λ_0 is the average stretch ratio of the end-to-end vector of a strand, λ_1 is the average stretch ratio of the end-to-end vector of a whole chain, $u_{ij} = |i-j|/N$, $Z = N/N_s$ denotes the average number of strands per chain, and μ is a numerical factor giving the rate of change of λ_{ij} as a function of u_{ij}. As seen from the above equation, λ_{ij} smoothly and monotonically increases from λ_0 to λ_1 as $|i-j|$ increases from N_s to N. A previous SANS study[8] suggests that the microscopic strain exhibits nonaffinity when $|i-j|$ is close to or a little larger than the separation of the "tube diameter" d. It depends on $|i-j|$ and recovers the affinity when $|i-j|$ is much larger than d. It is seen that eq 30 is qualitatively consistent with previous experimental observations. Equation 30 seems to be arbitrary. However, it can be found that the analysis result is not sensitive to the functional form of λ_{ij}. Other functions in which λ_{ij} monotonically approaches λ_1 from λ_0 as $|i-j|$ increases from N_s to N lead to similar analysis results.

The above model reflects the entanglement and spatial inhomogeneity of deformed polymers. Conceptually, it is similar to the classical theory for rubbers.[20−22] In the rubber elasticity theory, the stress tensor is determined by the average configuration of strands.[17] We assume that this conclusion also holds in our case. For the uniaxial extension problem, the tensile stress is of particular importance. With eq 28, one can find $\psi_2^0(i,j;\mathbf{r})$ and then calculate the tensile stress with eq 22 numerically. For the above model, due to its Gaussian form, the calculation of the tensile stress is analytical. It is straightforward to find that

$$\langle R_{s,x}R_{s,x}\rangle = \int {R_{s,x}}^2\left(\frac{\beta_s^2}{\pi}\right)^{3/2} \times \exp\left[-\beta_s^2\left(\lambda_0{R_{s,x}}^2 + \lambda_0{R_{s,y}}^2 + \frac{{R_{s,z}}^2}{{\lambda_0}^2}\right)\right] d\mathbf{R}_s = \frac{1}{2\lambda_0\beta_s^2} \tag{31}$$

$$\langle R_{s,z}R_{s,z}\rangle = \int {R_{s,z}}^2\left(\frac{\beta_s^2}{\pi}\right)^{3/2} \times \exp\left[-\beta_s^2\left(\lambda_0{R_{s,x}}^2 + \lambda_0{R_{s,y}}^2 + \frac{{R_{s,z}}^2}{{\lambda_0}^2}\right)\right] d\mathbf{R}_s = \frac{{\lambda_0}^2}{2\beta_s^2} \tag{32}$$

With the preceding two equations, one can find the tensile stress to be[17]

$$\sigma_{zz} - \sigma_{xx} = 2n_sk_BT\beta_s^2(\langle R_{s,z}R_{s,z}\rangle - \langle R_{s,x}R_{s,x}\rangle) = n_sk_BT\left({\lambda_0}^2 - \frac{1}{\lambda_0}\right) \tag{33}$$

where n_s is the number density of strands. In the rubber elasticity theory, n_sk_BT is just the elastic modulus G_e of the sample.[17] Then we can rewrite the preceding equation as

$$\sigma_{zz} - \sigma_{xx} = G_e\left({\lambda_0}^2 - \frac{1}{\lambda_0}\right) \tag{34}$$

III. SAMPLE AND EXPERIMENT

To investigate the chain conformation of deformed polymers, we carry out a series of SANS experiments on a polymeric system. The sample is a mixture of protonated (h-PS) and deuterated (d-PS) polystyrene homopolymers with a d/h ratio of 10/90 (h-PS: M_w = 197 kg/mol, M_w/M_n = 1.01; d-PS: M_w = 213 kg/mol, M_w/M_n = 1.06). The linear viscoelastic property of the sample is characterized by small-amplitude oscillatory shear measurements in the frequency range 0.1−100 rad/s and at temperatures between 124 and 184 °C on an HR2 rheometer (TA Instruments). The result at 124 °C, constructed by employing the time−temperature superposition principle, is plotted in Figure 2. The storage modulus $G'(\omega)$ exhibits a plateau, indicating the existence of entanglements in our sample.

DOI: 10.1021/acs.macromol.8b01913
Macromolecules 2018, 51, 9011−9018

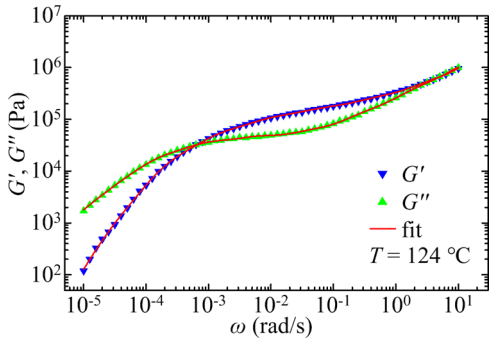

Figure 2. Frequency dependence of the storage and loss moduli G' and G'' of the sample at 124 °C (symbols). The solid lines denote the curves fitted with eq 35.

The plateau modulus, which is found to be 2×10^5 Pa from Figure 2, can be considered as an approximation of the elastic modulus G_e of the sample.

To describe the data of dynamic moduli and to estimate the longest relaxation time τ_t of the sample at isotropic state, we model the relaxation modulus by a discrete spectrum:[23,24]

$$G(t) = \sum_{i=1}^{N_r} g_i e^{-t/\tau_i} \tag{35}$$

where g_i and τ_i are the ith modulus and characteristic time, respectively. N_r is the number of relaxation modes and is set to be 8.[24] The fitted dynamic moduli are also shown in Figure 2. The longest relaxation time is evaluated by $\tau_t = \int_0^\infty G(s)s\,ds / \int_0^\infty G(s)\,ds$, and the result is found to be 6.8×10^3 s.

Two sets of deformed samples have been investigated. For sample set I, isotropic polymer melts were uniaxially stretched at 124 °C with a constant crosshead velocity $v = 8l_0/\tau_R$, where l_0 is the initial length of the sample and τ_R is the Rouse time calculated by the Osaki formula[25,26] [$\tau_R = (6M_w\eta/\pi^2\rho RT)(1.5M_e/M_w)^{2.4}$, where η is the zero-shear viscosity, M_e is the entanglement molecular weight, ρ is the mass density of the polymer, and R is the universal gas constant]. The extension was stopped at three macroscopic strains corresponding to stretch ratios of λ = 1.5, 1.8, and 2.4 and then immediately quenched to the glassy state with liquid nitrogen. For sample set II, the isotropic polymer melts were uniaxially stretched to λ = 1.8 at 124 °C with a constant crosshead velocity $v = 8l_0/\tau_R$ first. The samples were allowed to relax for different amount of time at 124 °C at the constant strain and then immediately quenched to the glassy state. In our experiments, <10 s was needed to decrease the temperature from 124 to 110 °C. This amount of time is smaller than τ_R at 124 °C by more than 1 order. Moreover, the molecular motion is considerably slowed well before the glass transition. Thus, we are confident that the quenching process well freeze the conformation of the polymer chain.

The SANS spectra of the quenched glassy samples were taken at the NGB30 SANS spectrometer at the NIST Center for Neutron Research. The wavelength of incident neutron was 6 Å. Two different sample-to-detector distances, 4 and 13 m, were chosen to cover a Q range from 0.006 to 0.1 Å^{-1}.

IV. RESULTS AND DISCUSSION

Model Fitting. The distribution function of the above-mentioned network model is summarized as follows:

$$\psi(i,j;\mathbf{r}) = \begin{cases} \left(\frac{3}{2\pi N_s b^2 w_{ij}}\right)^{3/2} \sqrt{\frac{1}{(w_{ij}/\lambda_0 + 1 - w_{ij})(w_{ij}/\lambda_0 + 1 - w_{ij})(w_{ij}\lambda_0^2 + 1 - w_{ij})}} \exp\left[-\frac{3}{2N_s b^2 w_{ij}}\left(\frac{r_x^2}{w_{ij}/\lambda_0 + 1 - w_{ij}} + \frac{r_y^2}{w_{ij}/\lambda_0 + 1 - w_{ij}} + \frac{r_z^2}{w_{ij}\lambda_0^2 + 1 - w_{ij}}\right)\right], & |i-j| \le N_s \\ \left(\frac{3}{2\pi N b^2 u_{ij}}\right)^{3/2} \exp\left[-\frac{3}{2Nb^2 u_{ij}}\left(\lambda_{ij} r_x^2 + \lambda_{ij} r_y^2 + \frac{r_z^2}{\lambda_{ij}^2}\right)\right], & |i-j| > N_s \end{cases} \tag{36}$$

where $w_{ij} = |i-j|/N_s$, $u_{ij} = |i-j|/N$, and

$$\lambda_{ij} = \lambda_0 + (\lambda_1 - \lambda_0)\left[1 - \exp\left(-\mu\frac{u_{ij} - 1/Z}{1 - u_{ij}}\right)\right], \quad |i-j| > N_s \tag{37}$$

In the preceding equations, N and N_s could be ambiguous since the description of the polymer by discretized segments is an artifact. Nb^2 can be replaced with $Nb^2 = 6R_{g,0}^2$, where $R_{g,0}^2$ is the mean-square radius of gyration of a polymer chain measured at isotropic state. In this study, $R_{g,0}^2$ is found to be 120^2 Å^2 by fitting the SANS spectrum of an isotropic sample with the Debye function. In addition, we use $Z = N/N_s$ instead of N_s to be a parameter. The value of Z is found to be 15 for the measured sample by $Z = G_e M_w/\rho RT$ (this relation is slightly different in different theories[3,27]).[18] Summarizing these ideas, it is found that only three parameters, λ_0, λ_1, and μ, need to be determined from the SANS experiment. λ_0 and λ_1 are crucial in characterizing the conformation of the chain and will be discussed in detail in the following parts. We would like to point out that the above considerations ignore the fluctuations of the entanglement points and the number of monomers in a strand. The validity should be checked by examining if the fitted values of λ_0 and λ_1 are quantitatively consistent with the data of macroscopic stress and strain.

With eqs 12 and 15, one can transform the distribution function $\psi(i,j;\mathbf{r})$ given by eq 36 into $S(\mathbf{Q})$ and then compare with the measured spectra. As pointed out in previous literature and above paragraphs, $S_2^0(Q)$ is the most relevant coefficient that reflects the deformation of polymers at molecular level and connects to the macroscopic rheological behaviors. Therefore, we fit the measured $S_2^0(Q)$ to determine the values of λ_0 and λ_1 for all samples. The fitting results are shown in Figure 3. As can be seen, the fitting quality is convincing. The fitting result of λ_1 is sensitive to the data of $S_2^0(Q)$ around the peak position, while the fitting result of λ_0 is sensitive to the data of $S_2^0(Q)$ at high Q.

λ_1 and Chain Conformation. In this nonaffine network model, λ_1 denotes the average stretch ratio of the end-to-end vector of the chain. The fitting results of λ_1 are shown in Figure 4. For sample set I, the results of λ_1 are seen to quantitatively agree with the values of the macroscopic strain λ, as given in Figure 4a. This is expected for following reasons: First of all, the stretch rate is high enough to induce the chain stretching.[14] Second, the quenching procedure was applied right after the sample was stretched to the desired λ, so that there is no time for λ_1 to relax (the influence of the relaxation taking place at

DOI: 10.1021/acs.macromol.8b01913
Macromolecules 2018, 51, 9011−9018

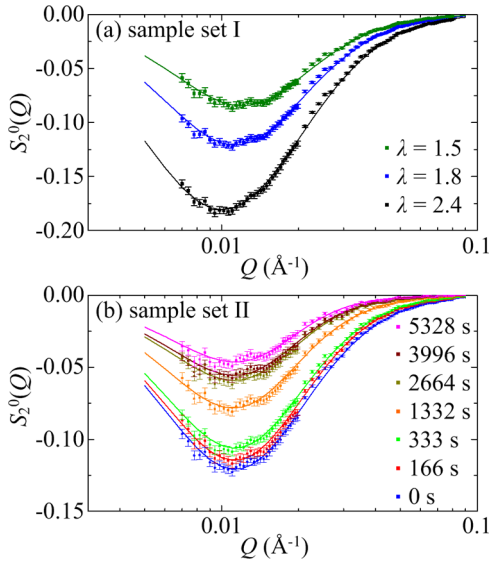

Figure 3. Panel a gives the measured $S_2^0(Q)$ (symbols) and the fitted curves (solid lines) for samples that have been stretched to λ = 1.5, 1.8, and 2.4 (sample set I). Panel b gives the relaxation of the measured $S_2^0(Q)$ (symbols) and the fitted curves (solid lines) after a large uniaxial step-strain with λ = 1.8 (sample set II).

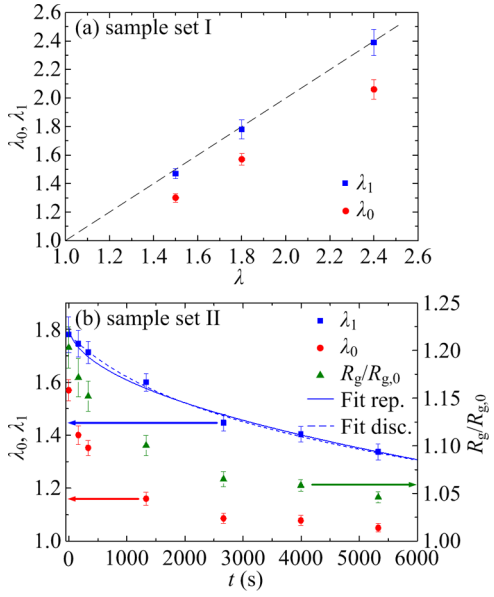

Figure 4. Panel a gives λ_0 and λ_1 as a function of the macroscopic stretch ratio λ (sample set I). The dashed line denotes the relation of $\lambda_1 = \lambda$. Panel b gives the relaxation of λ_0, λ_1, and R_g after a large uniaxial step strain with λ = 1.8 (sample set II). The solid line and dashed line denote the fitted curves with the reptation theory (eq 38) and the discrete-spectrum model, respectively.

the ends of the chain within seconds could be small for a well-entangled polymer). The excellent agreement between λ_1 and λ suggests that λ_1 is a proper microscopic quantity that characterizes the end-to-end vector of a single chain. This result could be of particular importance, since the evolution of the end-to-end vector of a single chain of deformed polymers is the centerpiece of many theories of polymer dynamics.[3,28,29] λ_0 is seen to be smaller than λ_1 from Figure 4a, which should be due to the relaxation of the chain at small length scales during the stretching process.

λ_0 and Stress. λ_0 represents the average strain of the strand in a network model. It determines the tensile stress of a uniaxially deformed network, as suggested by eq 34. Figure 5

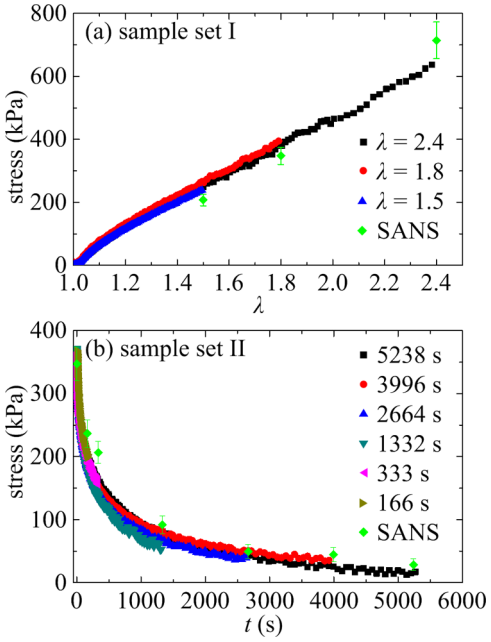

Figure 5. Panel a gives the tensile stress as a function of the macroscopic stretch ratio λ during the stretching process (sample set I). Panel b gives the relaxation of the tensile stress after a large uniaxial step strain with λ = 1.8 (sample set II). Green diamonds denote the results calculated with eq 34 in both panels.

gives the macroscopic stress measured by rheometry and the microscopic stress calculated by eq 34 for all samples. The two results exhibit similar behaviors as λ or the waiting time changes. This agreement may be unexpected because our network model does not contain any details about the entanglement and interchain effect. Nevertheless, the result shown in Figure 5 suggests that the fitting results of λ_0 provide a practical way to estimate the stress of entangled polymers with the SANS spectra from the viewpoint of rubber elasticity.

Relaxation. The relaxation of a whole chain plays a crucial role in determining the rheological behaviors of polymers. Thus, examining the chain relaxation at molecular level is of theoretical and practical importance. Figure 4b displays the relaxations of λ_1 and λ_0 for the stretched sample. The fitting result of μ is found to be around 1.6 for all cases in sample set II and does not exhibit any significant time dependence. Because λ_1 describes the end-to-end vector of the whole chain, its relaxation represents the longest relaxation process for a chain in our model. From Figure 4b it is seen that the relaxation of λ_1 is indeed much slower than that of λ_0. We also plot the relaxation of R_g, calculated with eq 19, in Figure 4b. The decay rate of R_g is found in between those of λ_1 and λ_0.

The relaxation of λ_1 can be evaluated by phenomenological models. We use the discrete-spectrum model given by eq 35 to fit the decay of λ_1 to isotropic state. With three relaxation modes, we find the relaxation time τ of λ_1 to be 8.9×10^3 s. Another trial was made by considering the reptation theory for entangled polymers.[2] In this picture, the relaxation of λ_1 reflects the disengagement of a chain. We tentatively fit $\lambda_1(t)$ with the equation of motion for classic reptation theory:[2]

DOI: 10.1021/acs.macromol.8b01913
Macromolecules 2018, 51, 9011−9018

$$\frac{\lambda_1(t) - 1}{\lambda_1(0) - 1} = \sum_{p:\text{odd}} \frac{8}{p^2\pi^2} \exp\left(-\frac{p^2 t}{\tau}\right) \quad (38)$$

The value of τ, extracted from the fit, is 8.0×10^3 s. The fitted curves from both models are plotted in Figure 4b. The fitting qualities are seen to be satisfactory. On the contrary, the decay of λ_0 cannot be well fitted by eq 38, as expected. For both models, τ is found to be larger than the longest relaxation time obtained from the linear rheology. Notice that recent SANS studies suggest that the classic tube theory is not complete in describing the dynamics of entangled polymers in nonlinear region.[15,16] The relaxation of the chain after a large step strain needs further investigations.

V. CONCLUSIONS

In this work, we conducted a series of SANS experiments on entangled polystyrene samples undergoing uniaxial deformation. The spherical harmonic expansion method with the extension to the real space was applied to decompose the 2D SANS spectrum into several 1D coefficients with specific physical meanings. We improved a network model by considering the nonaffinity of the deformation of entanglement points to interpret the SANS data. By analyzing the leading anisotropic coefficient $S_2^0(Q)$ and the isotropic coefficient $S_0^0(Q)$, we were able to extract the stretch ratio of the end-to-end vector and the radius of gyration of a single chain in deformed polymers. In addition, our method is found to provide a practical way to estimate the stress from the SANS spectra through the viewpoint of rubber elasticity.

AUTHOR INFORMATION

Corresponding Authors

*E-mail: mahw@dlut.edu.cn (H.M.).
*E-mail: zwang2017@mail.tsinghua.edu.cn (Z.W.).

ORCID

Hongwei Ma: 0000-0003-3897-9907
Yun Liu: 0000-0002-0944-3153
Zhe Wang: 0000-0003-4103-0751

Author Contributions

Z.-Y.W. and D.K. contributed equally.

Notes

The authors declare no competing financial interest.

ACKNOWLEDGMENTS

The research at Tsinghua University was supported by the Starting Grant from Tsinghua University. The sample synthesis, finished at Dalian University of Technology, was supported by the National Natural Science Foundation of China (No. 21674017). We acknowledge the support of the National Institute of Standards and Technology, U.S. Department of Commerce, in providing the neutron research facilities. Access to NGB30m SANS was provided by the Center for High Resolution Neutron Scattering, a partnership between the National Institute of Standards and Technology and the National Science Foundation under Agreement No. DMR-1508249. Certain commercial equipment, instruments, or materials (or suppliers, or software, ...) are identified in this paper to foster understanding. Such identification does not imply recommendation or endorsement by the National Institute of Standards and Technology, nor does it imply that the materials or equipment identified are necessarily the best available for the purpose. Finally, Z.W. thanks Dr. Yangyang Wang (Oak Ridge National Laboratory) for the discussion on the calculation of stress.

REFERENCES

(1) Higgins, J. S.; Benoît, J. C. *Polymers and Neutron Scattering*; Clarendon: Oxford, England, 1994.
(2) de Gennes, P. G. Reptation of a polymer chain in the presence of fixed obstacles. *J. Chem. Phys.* **1971**, *55*, 572−579.
(3) Doi, M.; Edwards, S. F. *The Theory of Polymer Dynamics*; Clarendon: Oxford, England, 1986.
(4) Straube, E.; Urban, V.; Pyckhout-Hintzen, W.; Richter, D. SANS investigations of topological constraints and microscopic deformations in rubberelastic networks. *Macromolecules* **1994**, *27*, 7681−7688.
(5) Straube, E.; Urban, V.; Pyckhout-Hintzen, W.; Richter, D.; Glinka, C. J. Small-angle neutron scattering investigation of topological constraints and tube deformation in networks. *Phys. Rev. Lett.* **1995**, *74*, 4464−4467.
(6) Westermann, S.; Urban, V.; Pyckhout-Hintzen, W.; Richter, D.; Straube, E. SANS investigations of topological constraints in networks made from triblock copolymers. *Macromolecules* **1996**, *29*, 6165−6174.
(7) Westermann, S.; Pyckhout-Hintzen, W.; Richter, D.; Straube, E.; Egelhaaf, S.; May, R. On the length scale dependence of microscopic strain by SANS. *Macromolecules* **2001**, *34*, 2186−2194.
(8) Pyckhout-Hintzen, W.; Botti, A.; Heinrich, M.; Westermann, S.; Richter, D.; Straube, E. The length-scale dependence of strain in networks by SANS. *Appl. Phys. A: Mater. Sci. Process.* **2002**, *74*, S368−S370.
(9) Blanchard, A.; Graham, R. S.; Heinrich, M.; Pyckhout-Hintzen, W.; Richter, D.; Likhtman, A. E.; McLeish, T. C. B.; Read, D. J.; Straube, E.; Kohlbrecher, J. Small-angle neutron scattering observation of chain retraction after a large step deformation. *Phys. Rev. Lett.* **2005**, *95*, 166001.
(10) Boué, F.; Nierlich, M.; Jannink, G.; Ball, R. Polymer coil relaxation in uniaxially strained polystyrene observed by small angle neutron scattering. *J. Phys. (Paris)* **1982**, *43*, 137−148.
(11) Boué, F.; Nierlich, M.; Osaki, K. Dynamics of molten polymers on the sub-molecular scale-application of small-angle-neutron-scattering to transient relaxation. *Faraday Symp. Chem. Soc.* **1983**, *18*, 83−105.
(12) Ullman, R. Small angle neutron scattering from polymer networks. *J. Chem. Phys.* **1979**, *71*, 436−449.
(13) Ullman, R. Small-angle neutron scattering from elastomeric networks. Application to labeled chains containing several cross-links. *Macromolecules* **1982**, *15*, 1395−1402.
(14) Hassager, O.; Mortensen, K.; Bach, A.; Almdal, K.; Rasmussen, H. K.; Pyckhout-Hintzen, W. Stress and neutron scattering measurements on linear polymer melts undergoing steady elongational flow. *Rheol. Acta* **2012**, *51*, 385−394.
(15) Wang, Z.; Lam, C. N.; Chen, W.-R.; Wang, W.; Liu, J.; Liu, Y.; Porcar, L.; Stanley, C. B.; Zhao, Z.; Hong, K.; Wang, Y. Fingerprinting molecular relaxation in deformed polymers. *Phys. Rev. X* **2017**, *7*, 031003.
(16) Lam, C. N.; Xu, W.-S.; Chen, W.-R.; Wang, Z.; Stanley, C. B.; Carrillo, J.-M. Y.; Uhrig, D.; Wang, W.; Hong, K.; Liu, Y.; Porcar, L.; Do, C.; Smith, G. S.; Sumpter, B. G.; Wang, Y. Scaling behavior of anisotropic relaxation in deformed polymers. *Phys. Rev. Lett.* **2018**, *121*, 117801.
(17) Larson, R. G. *Constitutive Equations for Polymer Melts and Solutions*; Butterworths: Stoneham, MA, 1988.
(18) Ferry, J. D. *Viscoelastic Properties of Polymers*, 3rd ed.; Wiley: New York, 1980.
(19) Maconnachie, A.; Allen, G.; Richards, R. W. Small-angle neutron scattering from a polymer coil undergoing stress relaxation. *Polymer* **1981**, *22*, 1157−1160.

DOI: 10.1021/acs.macromol.8b01913
Macromolecules 2018, 51, 9011−9018

(20) Flory, P. J.; Rehner, J. Statistical mechanics of cross-linked polymer networks I. rubberlike elasticity. *J. Chem. Phys.* **1943**, *11*, 512−520.
(21) James, H. M.; Guth, E. Theory of the elastic properties of rubber. *J. Chem. Phys.* **1943**, *11*, 455−481.
(22) Green, M. S.; Tobolsky, A. V. A new approach to the theory of relaxing polymeric media. *J. Chem. Phys.* **1946**, *14*, 80−92.
(23) Baumgaertel, M.; Winter, H. H. Determination of discrete relaxation and retardation time spectra from dynamic mechanical data. *Rheol. Acta* **1989**, *28*, 511−519.
(24) Baumgaertel, M.; Schausberger, A.; Winter, H. H. The relaxation of polymers with linear flexible chains of uniform length. *Rheol. Acta* **1990**, *29*, 400−408.
(25) Osaki, K.; Uematsu, T.; Yamashita, Y. Evaluation methods of the longest Rouse relaxation time of an entangled polymer in a semidilute solution. *J. Polym. Sci., Part B: Polym. Phys.* **2001**, *39*, 1704−1712.
(26) Osaki, K.; Nishizawa, K.; Kurata, M. Material time constant characterizing the nonlinear viscoelasticity of entangled polymeric systems. *Macromolecules* **1982**, *15*, 1068.
(27) Likhtman, A. E.; McLeish, T. C. Quantitative theory for linear dynamics of linear entangled polyers. *Macromolecules* **2002**, *35*, 6332−6343.
(28) Rouse, P. E. A theory of the linear viscoelastic properties of dilute solutions of coiling polymers. *J. Chem. Phys.* **1953**, *21*, 1272−1280.
(29) Zimm, B. H. Dynamics of polymer molecules in dilute solution: Viscosity, flow birefringence and dielectric loss. *J. Chem. Phys.* **1956**, *24*, 269−278.

DOI: 10.1021/acs.macromol.8b01913
Macromolecules 2018, 51, 9011−9018